Supplementary Materials

Pressure-induced superconductivity in hypercoordinated 5*p*-block element nitrides MN_6 (M = Sb, Te, I)

Yan Liu[1], Da Li[1], Tian Cui[1,2]

[1]State Key Laboratory of Superhard Materials, College of Physics, Jilin University, Changchun 130012, Jilin, China.
[2]School of Physical Science and Technology, Ningbo University, Ningbo 315211, Zhejiang, China.

Correspondence to: Prof. Da Li, State Key Laboratory of Superhard Materials, College of Physics, Jilin University, 2699 Qianjin Street, Changchun 130012, Jilin, China. E-mail: dali@jlu.edu.cn; Prof. Tian Cui, School of Physical Science and Technology, Ningbo University, 818 Fenghua Road, Ningbo 315211, Zhejiang, China. E-mail: cuitian@nbu.edu.cn

Table of Content

Supplementary computational details

Structure prediction

High-pressure structural predictions for the candidate structures were based on a global minimization of free energy surfaces merging ab initio total-energy calculations via particle swarm optimization (PSO) algorithm as implemented in the Crystal structure AnaLYsis by Particle Swarm Optimization (CALYPSO) code[1,2]. The CALYPSO method unbiased by any known structural information has been benchmarked on various known systems and successfully predicted a great of high-pressure structures[3-6].

Structure simulations were performed at 20~200 GPa and the different stoichiometry of M_xN_y (M = Sb, Te, I) were searched with simulation cell sizes of 1~4 formula units (f.u.). The first generation is produced randomly with symmetry constraint (230 space group), and local optimization can drive the energy of the candidate structures to the local minimum. Then, the structures with the lowest enthalpy (70%) were selected to produce the next-generation structures by PSO, and 30% of the structures in the new generation were randomly generated. Symmetry checking has also been used to strictly prohibit the appearance of identical symmetric structures. The conjugate gradients method was used to perform local optimization and it was stopped when the enthalpy changes became smaller than 1×10^{-5} eV per atom. In most cases, the structure searching simulation reaches the convergence after 30~40 generations covering about 1,000~1,500 structures.

For Sb–N, Te–N, and I–N systems, a number of lowest enthalpy structures were selected and optimized as a function of pressures using the Vienna ab initio simulation (VASP) code[7,8]. The cutoff energy for the expansion of wavefunctions into the plane was set to 400 eV and the Monkhorst-Pack grid was generated with a reciprocal space resolution of $2\pi \times 0.03$ Å^{-1}. This usually gave well-converged total energies (within 1 meV per atom).

Supplementary Figures

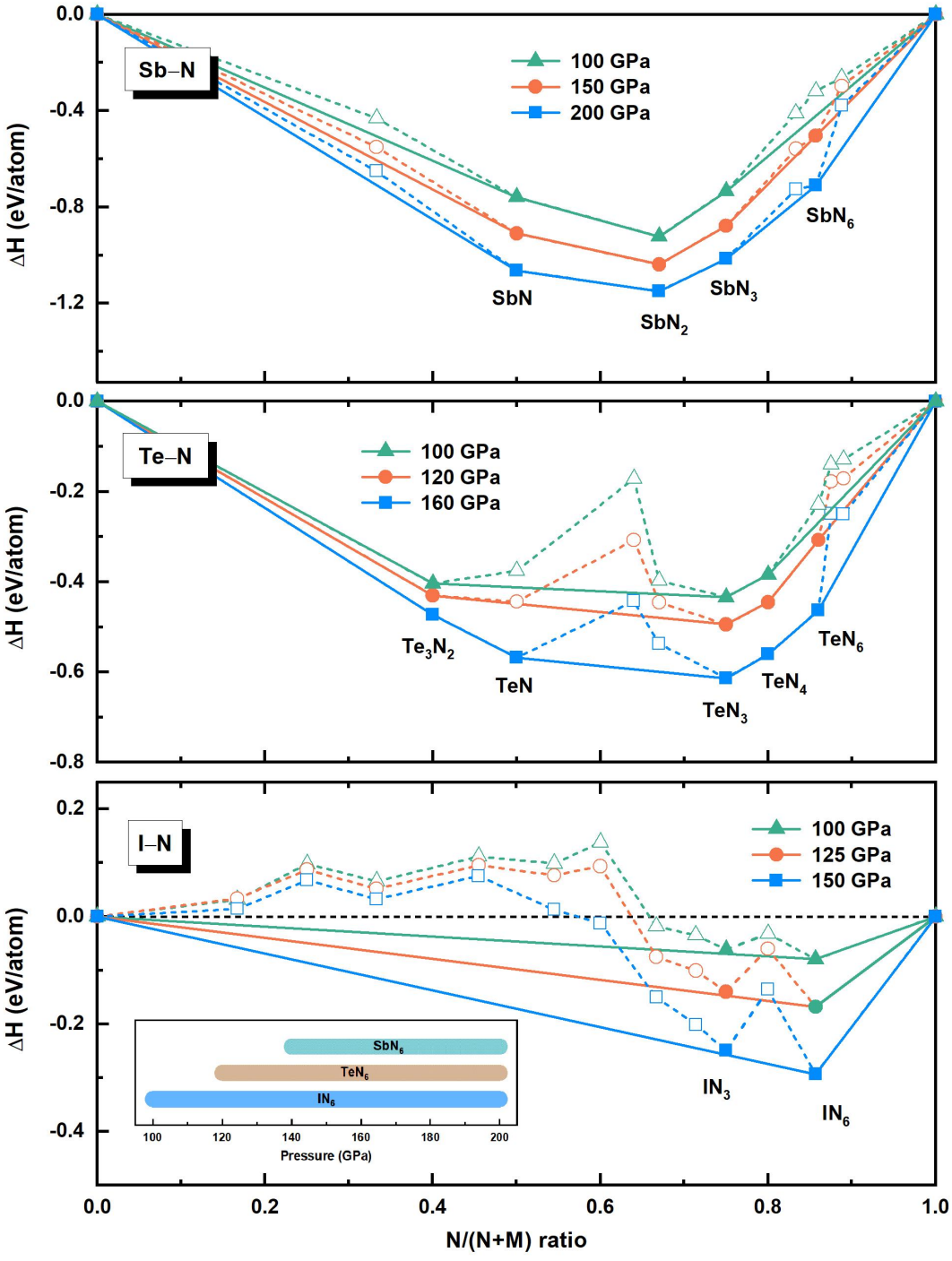

Supplementary Figure 1. Formation enthalpies of various 5*p*-block element nitrides under high pressure. The dotted lines connect the lowest formation enthalpy data points, and the solid lines denote the convex hull. The stable pressure ranges for SbN_6, TeN_6, and IN_6 are shown in the insets.

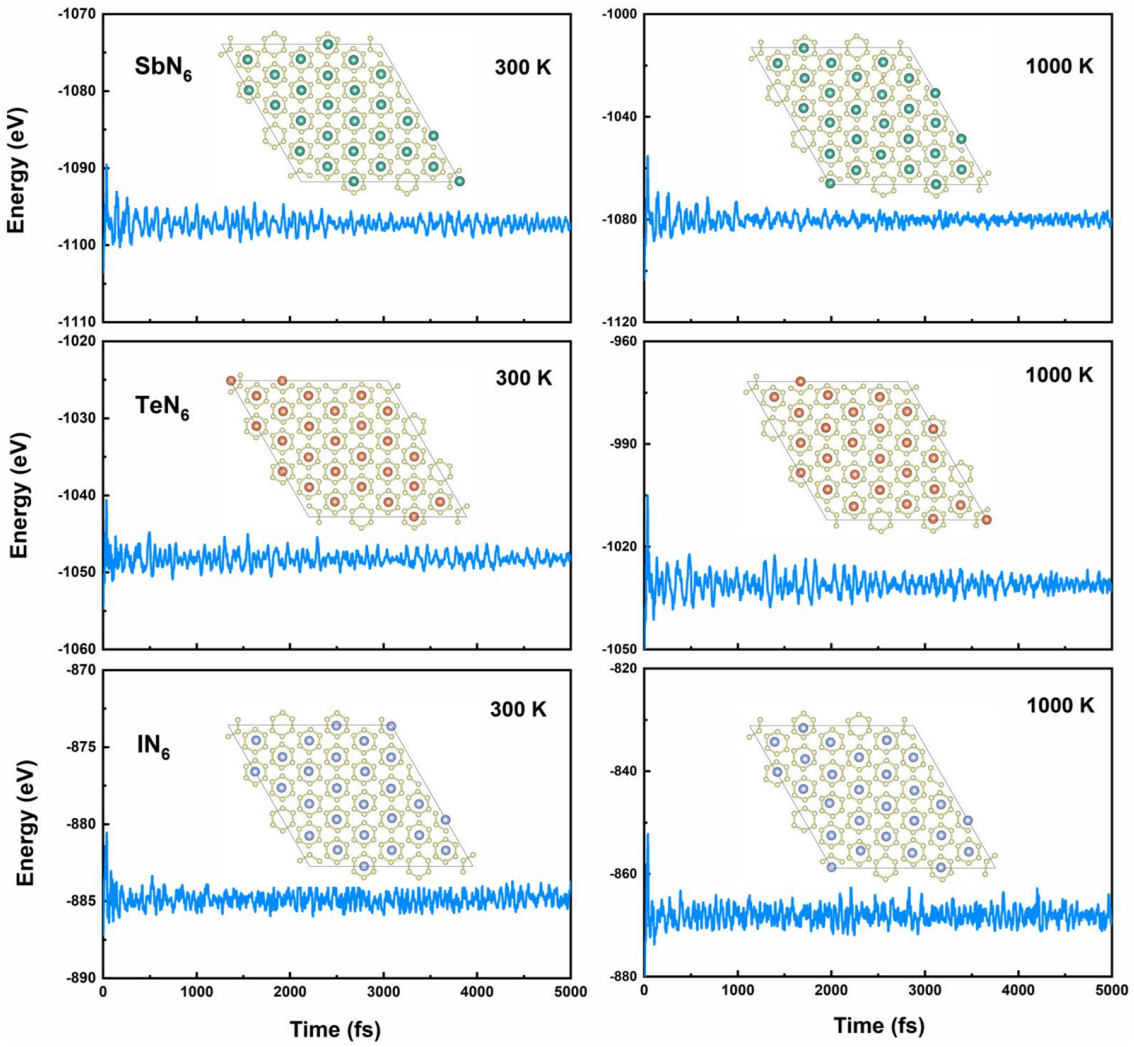

Supplementary Figure 2. Molecular dynamic simulations (AIMD) of 5*p*-block element nitrides MN_6 (M = Sb, Te, I) at different chemical potentials at 300 K and 1,000 K for 5,000 fs. Insets in each figure are structure snapshots of the AIMD simulation at 5,000 fs, the structural framework remains basically unchanged after a typically long simulation time, demonstrating the superb thermal stability of MN_6.

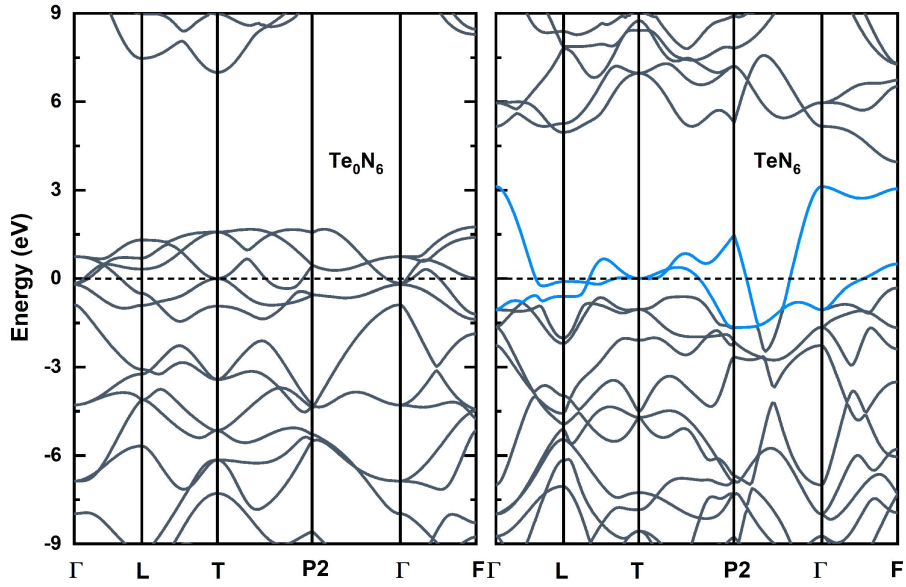

Supplementary Figure 3. Electron band structure of Te_0N_6 (left) and TeN_6 (middle) at 100 GPa. There are two conduction bands that are half-filled in Te_0N_6. Horizontal dotted lines indicate the Fermi level.

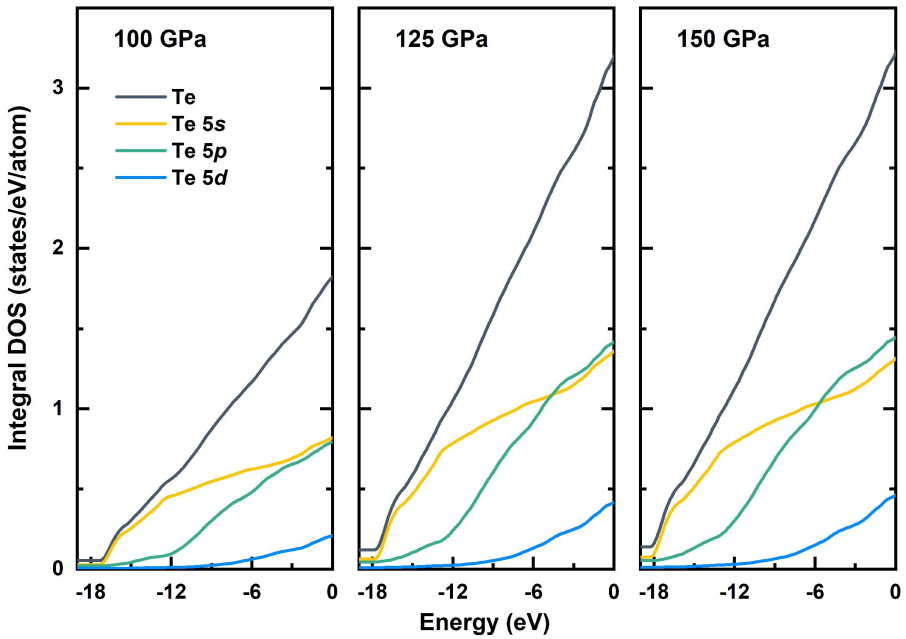

Supplementary Figure 4. Integral DOS values of atomic Te at different pressure. The total number of electronic states occupied by atomic Te gradually increases under compression, but the content of occupied 5*s*, 5*p*, and 5*d* states are quite different.

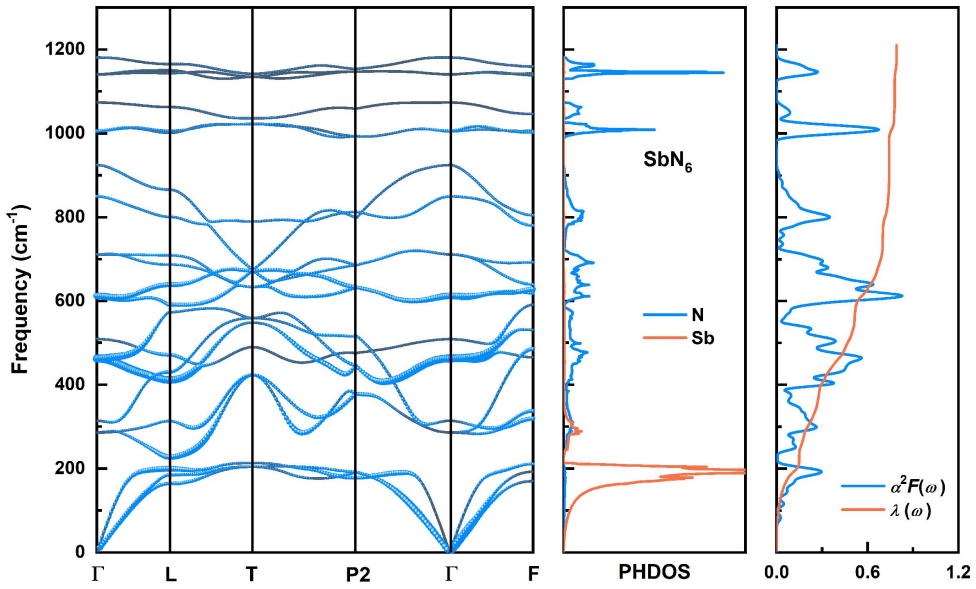

Supplementary Figure 5. Phonon band structure, phonon density of state (PHDOS), Eliashberg spectral function $\alpha^2F(\omega)$ and integral electron-phonon coupling parameter $\lambda(\omega)$ of SbN_6 at 100 GPa.

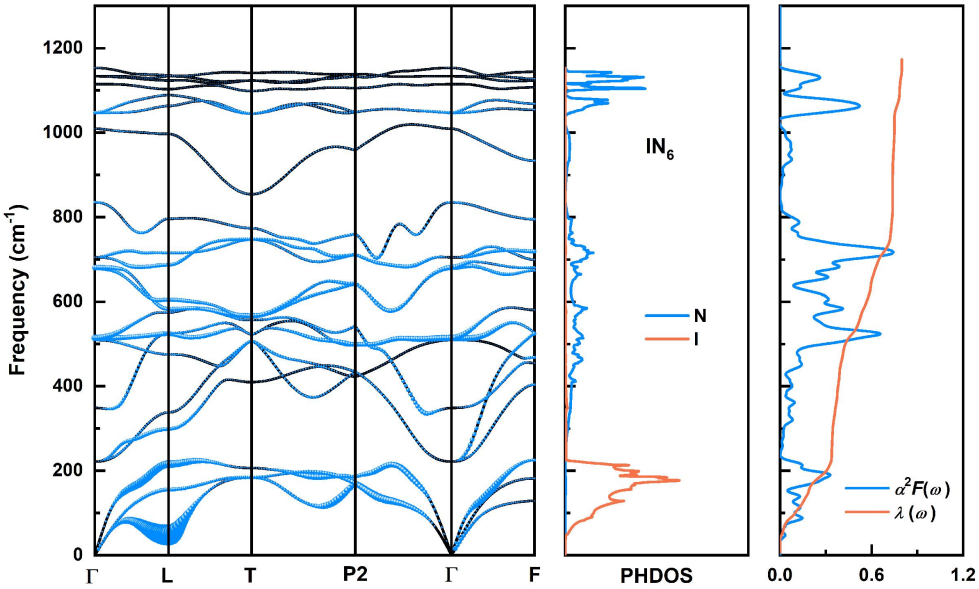

Supplementary Figure 6. Phonon band structure, phonon density of state (PHDOS), Eliashberg spectral function $\alpha^2F(\omega)$ and integral electron-phonon coupling parameter $\lambda(\omega)$ of IN_6 at 100 GPa.

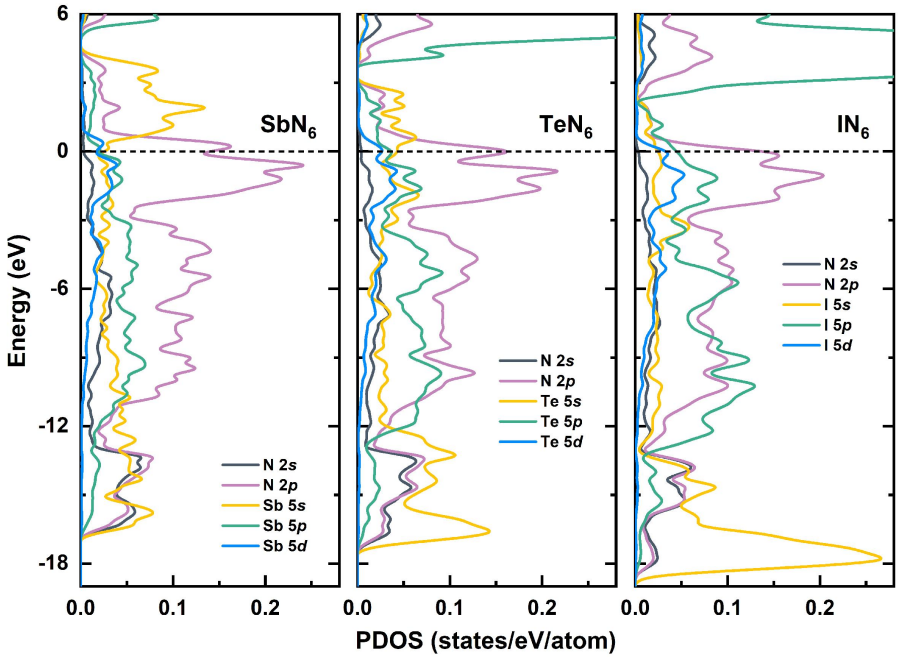

Supplementary Figure 7. Projected density of states (PDOS) of 5*p*-block element nitrides MN_6 (M = Sb, Te, I) at 100 GPa. Horizontal dotted lines indicate the Fermi level.

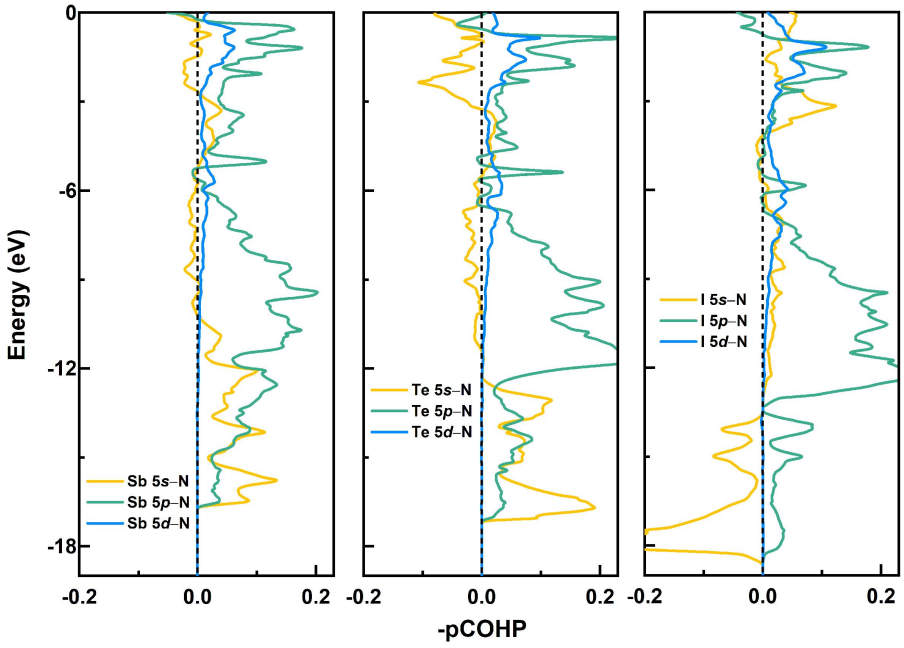

Supplementary Figure 8. Projected Crystal orbital Hamilton population (pCOHP) of 5*p*-block element nitrides MN_6 (M = Sb, Te, I) at 100 GPa. All of them show the M–N covalent bonding characteristic.

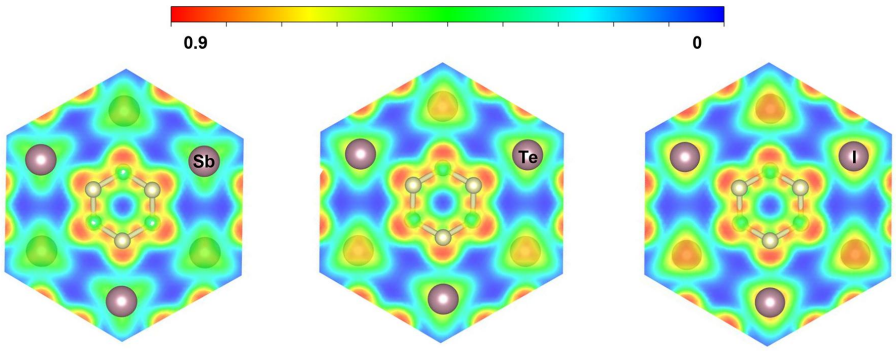

Supplementary Figure 9. Electron localization function (ELF) of 5*p*-block element nitrides MN_6 (M = Sb, Te, I) at 100 GPa. All of them show the M–N covalent bonding characteristic.

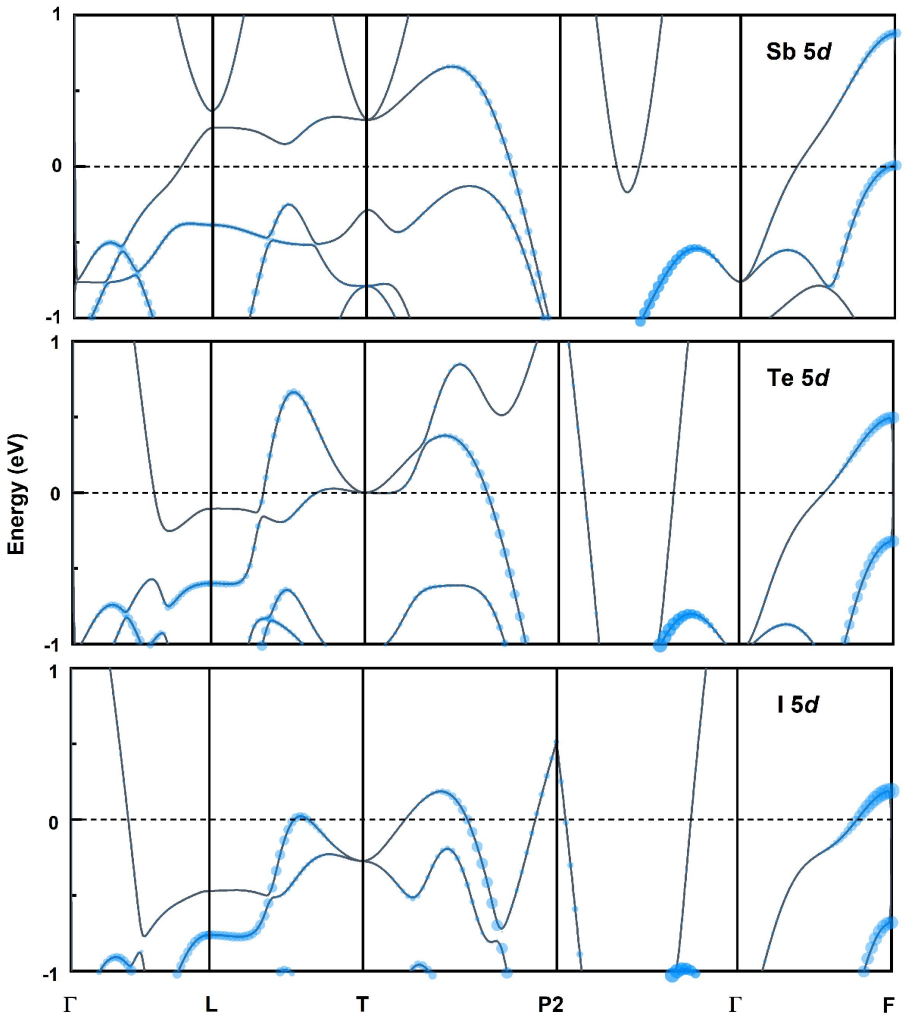

Supplementary Figure 10. Projected electron band structure of 5*p*-block element nitrides MN_6 (M = Sb, Te, I) at 100 GPa.

Supplementary Tables

Supplementary Table 1. Structure information of the stable 5*p*-block element nitrides MN_6 (M = Sb, Te, I)

Structure	Pressure (GPa)	Lattice parameters (Å, °)	Atom	X	Y	Z
SbN_6	100	a = 3.692	N (6h)	-0.311	-0.311	-0.673
		α = 104.871	Sb (1a)	0.000	0.000	0.000
TeN_6	100	a = 3.719	N (6h)	-0.677	-0.687	-0.325
		α = 105.358	Te (1a)	0.000	0.000	0.000
IN_6	100	a = 3.729	N (6h)	-0.677	-0.315	-0.315
		α = 105.845	I (1a)	0.000	0.000	0.000

Supplementary Table 2. Calculated Elastic Constants C_{ij} of 5*p*-block element nitrides MN_6 (M = Sb, Te, I) at 100 GPa

Structure	C_{11}	C_{33}	C_{44}	C_{12}	C_{13}	C_{14}
SbN_6	937.3	934.8	300.7	374.2	313.3	-3.45
TeN_6	963.3	1018.7	319.6	341.6	244.4	-8.7
IN_6	1116.1	1123.2	377.6	317.7	195.3	-27.9

The simple mechanical stability criteria of a rhombohedral phase is given by $C_{44} > 0$, $C_{11} > |C_{12}|$, $C^2_{13} < 1/2\ C_{33}\ (C_{11} + C_{12})$, and $C^2_{14} < 1/2\ C_{44}\ (C_{11} - C_{12}) \equiv C_{44}\ C_{66}$.

Supplementary Table 3. Calculated pressure variation of electron density of states at E_F $N(\varepsilon_F)$, logarithmic average phonon frequency ω_{log}, Hopfield parameter η, electron-phonon coupling parameter λ, and superconducting critical temperature T_c for $\mu^* = 0.10$ (0.13) in 5*p*-block element nitrides MN_6 (M = Sb, Te, I)

Structure	Pressure (GPa)	$N(\varepsilon_F)$ (states/spin/eV)	η	ω_{log} (K)	λ	T_c (K)
SbN_6	100	6.86	0.12	618	0.79	28.4 (22.9)
	125	6.61	0.10	674	0.69	22.9 (17.5)
	150	6.49	0.09	717	0.63	19.2 (14.0)
TeN_6	100	7.32	0.15	517	1.01	36.8 (31.7)
	125	6.73	0.12	650	0.78	28.6 (22.9)
	150	6.17	0.10	734	0.65	20.8 (15.3)
IN_6	100	5.62	0.14	473	0.80	22.1 (17.9)
	125	5.19	0.12	614	0.62	15.3 (11.0)
	150	4.75	0.11	713	0.51	9.2 (5.6)

Supplementary Table 4. Selected N–N and Te–N bond lengths and average ICOHP values in the structure of TeN_6 at different pressure

Pressure (GPa)	Bond	Bond length (Å)	Average ICOHP (eV/pair)
100	N–N	1.37	-12.66
	Te–N	2.28	-2.18
	Te 5d–N		-0.23
125	N–N	1.357	-12.79
	Te–N	2.25	-2.31
	Te 5d–N		-0.24
150	N–N	1.35	-12.91
	Te–N	2.22	-2.44
	Te 5d–N		-0.25

Supplementary Table 5. The superconductivity dependence on pressure of the reported binary superconducting nitrides including SbN_6, TeN_6, and IN_6 proposed in this work

Structure	Pressure (GPa)	T_c (K)	Ref.
NbN	0	17.3	[9]
B_4N	0	0.59	[10]
Nb_4N_3	0	12.2	[11]
CoN	0	16.1	[12]
ZrN	0	9.73	[13]
HfN	0	8.83	[13]
AlN_6	0	18.9	[14]
OsN_2	0	1	[15]
CuN	5	32.45	[16]
PN_3	10	18	[17]
MoN	10	14	[18]
MnN_4	40	1.6	[19]
ZnN_2	50	0.01	[20]
Pt_3N_4	50	3.6	[21]
N_4H	72	37.7	[22]
SbN_6	100	28.4	This work
TeN_6	100	36.8	This work
IN_6	100	22.1	This work
ZnN_3	100	16.3	[23]
Li_5N	150	48.97	[24]
FeN_2	250	8	[25]

REFERENCES

1. Wang YC, Lv J, Zhu L, and Ma YM. CALYPSO: A method for crystal structure prediction. *Comput Phys Commun* 2012;183:2063. DOI: 10.1016/j.cpc.2012.05.008

2. Wang YC, Lv J, Zhu L, and Ma YM. Crystal structure prediction via particle-swarm optimization. *Phys Rev B* 2010;82:094116. DOI: 10.1103/PhysRevB.82.094116

3. Zhu L, Wang H, Wang Y et al. Substitutional alloy of Bi and Te at high pressure. *Phys Rev Lett* 2011;106:145501. DOI: 10.1103/PhysRevLett.106.145501

4. Liu Y, Cui T, and Li D. Emerging *d*−*d* orbital coupling between non-*d*-block main-group elements Mg and I at high pressure. *iScience* 2023;26:106113. DOI: 10.1016/j.isci.2023.106113

5. Lin JY, Zhao ZY, Liu CY et al. IrF_8 Molecular Crystal under High Pressure. *J Am Chem Soc* 2019;141:5409. DOI: 10.1021/jacs.9b00069

6. Luo DB, Lv J, Peng F et al. A hypervalent and cubically coordinated molecular phase of IF_8 predicted at high pressure. *Chem Sci* 2019;10:2543. DOI: 10.1039/C8SC04635B

7. Gonze X and Lee C. Dynamical matrices, Born effective charges, dielectric permittivity tensors, and interatomic force constants from density-functional perturbation theory. *Phys Rev B* 1997;55:10355. DOI: 10.1103/PhysRevB.55.10355

8. Kohn W and Sham LJ. Self-consistent equations including exchange and correlation effects. *Phys Rev* 1965;140:A1133. DOI: 10.1103/PhysRev.140.A1133

9. Rietschel H, Winter H, and Reichardt W. Strong depression of superconductivity in VN by spin fluctuations. *Phys Rev B* 1980;22:4284. DOI: 10.1103/PhysRevB.22.4284

10. Wang LY, Sun RX, Liu WH et al. Novel superhard boron-rich nitrides under pressure. *Sci China Mater* 2020;63:2358. DOI: 10.1007/s40843-020-1388-1

11. Kaiser R, Spengler W, Schicktanz S, and Politis C. Raman Spectra and Superconductivity of Various Phases of a High-T_c Superconductor: NbN. *Phys Status Solidi B* 1978;87:565. DOI: 10.1002/pssb.2220870220

12. Li Q and Chen LG. Superconducting atmospheric structure and pressure-induced novel phases of cobalt mononitride. *Comput Mater Sci* 2020;174:109464. DOI: 10.1016/j.commatsci.2019.109464

13. Maksimov EG, Wang SQ, Magnitskaya MV, and Ebert SV. Effect of high pressure on the phonon spectra and superconductivity in ZrN and HfN. *Supercond Sci Technol*

2009;22:075004. DOI: 10.1088/0953-2048/22/7/075004
14. Du HF, Ge YF, Zhu JL, Guo W, and Yao YG. Pressure-induced novel nitrogen-rich aluminum nitrides: AlN_6, Al_2N_7 and AlN_7 with polymeric nitrogen chains and rings. *Physical chemistry chemical physics : PCCP* 2021;23:12350. DOI: 10.1039/D1CP01027A
15. Hernández AD, Montoya JA, Profeta G, and Scandolo S. First-principles investigation of the electron-phonon interaction in OsN_2: Theoretical prediction of superconductivity mediated by N-N covalent bonds. *Phys Rev B* 2008;77:092504. DOI: 10.1103/PhysRevB.77.092504
16. Liao ZH, Yi XW, You JY, Gu B, and Su G. Family of binary transition metal pnictide superconductors. *Phys Rev B* 2022. DOI: 10.1103/PhysRevB.108.014501
17. Raza Z, Errea I, Oganov AR, and Saitta AM. Novel superconducting skutterudite-type phosphorus nitride at high pressure from first-principles calculations. *Scientific reports* 2014;4:5889. DOI: 10.1038/srep05889
18. Inumaru K, Nishikawa T, Nakamura K, and Yamanaka S. High-Pressure Synthesis of Superconducting Molybdenum Nitride δ-MoN by in Situ Nitridation. *Chem Mater* 2008;20:4756. DOI: 10.1021/cm800820d
19. Li L, Bao K, Zhao XB, and Cui T. Bonding Properties of Manganese Nitrides at High Pressure and the Discovery of MnN_4 with Planar N_4 Rings. *J Phys Chem C* 2021;125:24605. DOI: 10.1021/acs.jpcc.1c06730
20. Andrews NLP, Fan JZ, Forward RL, Chen MC, and Loock HP. Determination of the thermal, oxidative and photochemical degradation rates of scintillator liquid by fluorescence EEM spectroscopy. *Physical chemistry chemical physics : PCCP* 2017;19:73. DOI: 10.1039/C6CP06015C
21. Feng QC, Xiao X, Dai W et al. Predicted the structural diversity and electronic properties of Pt−N compounds under high pressure. *J Phys Condens Matter* 2023;35:285501. DOI: 10.1088/1361-648X/acccc5
22. Dai W, He S, Ding KW, and Lu C. Polymeric hydronitrogen N_4H: A promising high-energy-density material and high-temperature superconductor. *ACS Appl Mater Interfaces* 2022;14:49986. DOI: 10.1021/acsami.2c16293
23. Du HF and Guo W. Novel polymerization of nitrogen in zinc nitrides at high pressures. *J Phys Condens Matter* 2022;34:235702. DOI: 10.1088/1361-648X/ac5e76

24. Wan ZY, Zhang C, Yang TY, Xu WJ, and Zhang RQ. Predicted superconductivity and superionic state in the electride Li_5N under high pressure. *New J Phys* 2022;24:113012. DOI: 10.1088/1367-2630/ac9cff
25. Chen YZ, Cai XY, Wang HG, Wang HB, and Wang H. Novel triadius-like N_4 specie of iron nitride compounds under high pressure. *Scientific reports* 2018;8:10670. DOI: 10.1038/s41598-018-29038-w